Topic 7: Digital Reconstruction

7.1 Introduction

In image reconstruction the aim is to remove or compensate for the imaging system aberrations and try and reform the *ideal* image being the image that would have been detected if the system was perfect. The simplest cases is where the imaging system is *linear* and *space invariant* so that the aberrations can be characterised by its *Point Spread Function.* This is just the image *of a point* so typically can be directly measured or deuces form the system design, and thus known or at least a good approximation is known. These assumptions valid for a large range of practical systems

If we can assume this, then we have a linear convolution model for image formation where the detected, digital image $g(i,j)$ is

$$g(i,j) = f(i,j) \odot h(i,j) + n(i,j)$$

where $h(i,j)$ is the point spread function, $f(i,j)$ the *ideal* image and $n(i,j)$ the, assumed, additive noise, which is most cases we will assume is Gaussian zero meaned noise which is uncorrelated with the image[1]. In all practical reconstruction system we require to know, or have a good guess for $h(i,j)$ to get a good reconstruction. The general problem is that we detect $g(i,j)$ and wish to recover $f(i,j)$.

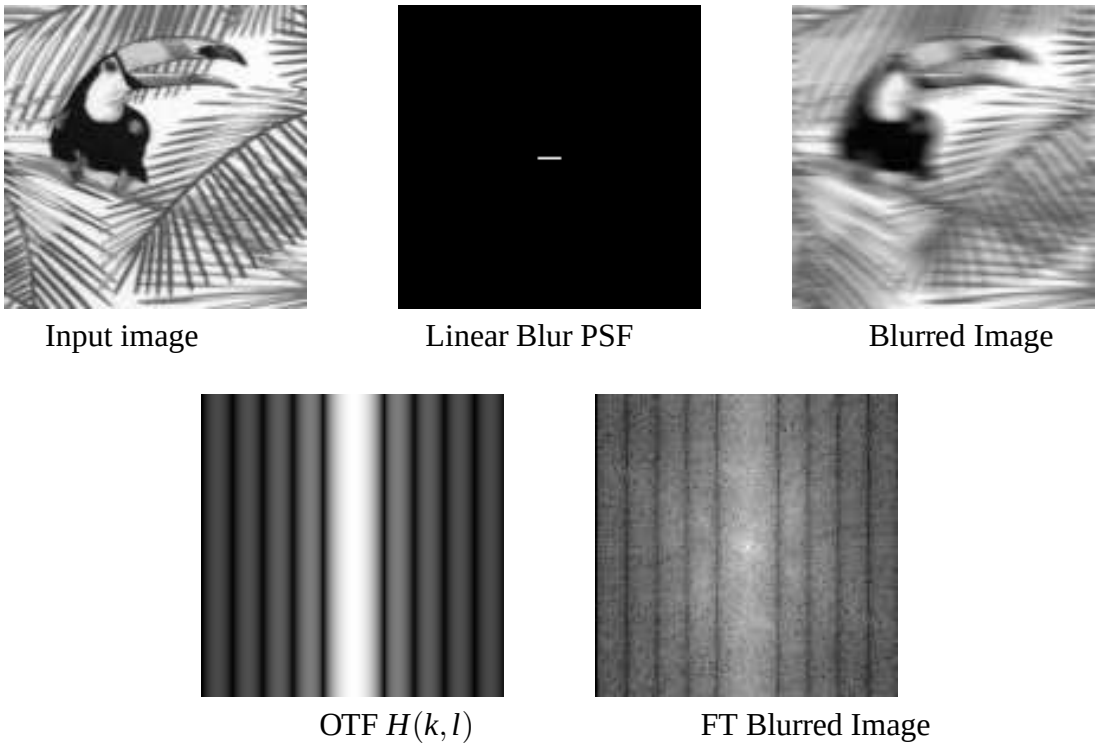

Figure 1: Example of a simulated linear blue of 9 pixels in both real and Fourier space.

The example of a linear blur is shown in figure 1 where the point spread function become a horizontal line of 9 pixels. This is the point spread function that would result from a horizontal translation of the camera during the exposure, and results in the image being horizontally

[1]Other noise models are possible, but vastly complicate the reconstruction process.

smudged. Here the $H(k,l)$ the optical transfer function has a characteristic sinc() profile in the horizontal direction, which is also seen in the Fourier transform of the blurred image.

Input image

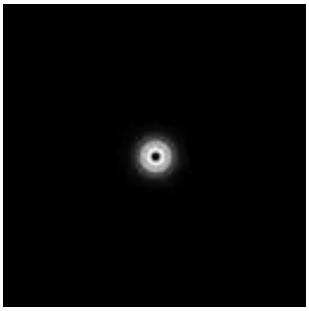

Defocus PSF

Defocused Image

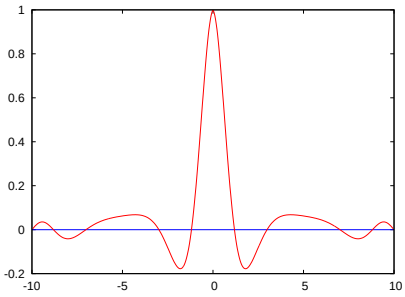

OTF $H(k,l)$

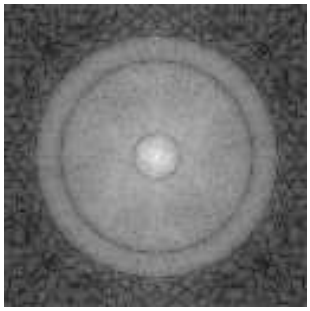

FT Defocused Image

Figure 2: Example of simulated defocus in both real and Fourier space.

The effect of the more common, and more complex, aberration of defocus is shown in figure 2 where for this extent of defocus the point spread function has a dark rather than bright centre. The optical transfer function, shown as a plot along the *k* axis shown a severe low-pass filtering effect with multiple zeros and *negative* regions where the contrast at that spatial frequency has been reversed. This results in a severely blurred image where most of the high frequency information appear to have been *lost*. However as we will see in this section, that even with a severe blur like this, provided we know the point spread function, reconstruction is still possible.

7.2 Inverse Filtering

The simplest scheme to recovering $f(i,j)$ having detected $g(i,j)$, is simple inverse filtering. Due the the convolution relation in real space, in Fourier space we have that

$$G(k,l) = F(k,l)\,H(k,l) + N(k,l)$$

where,since we know $h(i,j)$ we know, or can calculate $H(k,l)$, therefore the simplest estimate for Fourier transform of the ideal image is given by

$$\tilde{F}(k,l) = \frac{G(k,l)}{H(k,l)} = F(k,l) + \frac{N(k,l)}{H(k,l)}$$

where, clearly if $N(k,l) = 0$, then we have a exact solution, so problem solved, since we can simply inverse transform to get $f(i,j)$ the idea image.

This scheme has a major problem since even for tiny amounts of noise, $n(i,j)$ being Gaussian random noise, then

$$\langle |N(k,l)|^2 \rangle \approx \text{constant}$$

at all spatial frequencies, which as shown in figure 3, even for an ideal imaging system, $H(k,l) \to 0$ at high spatial frequencies. So the term will dominate at high frequencies and corrupt the reconstruction.

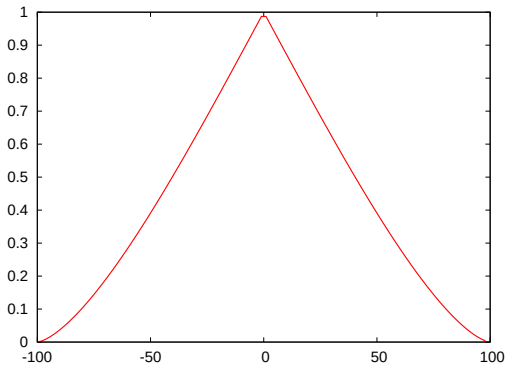

Figure 3: Plot of the Optical Transfer Function of an ideal imaging system.

In practice the situation is worse than this, since all system where reconstruction is needed, $H(k,l)$ will have multiple zeros and negative regions as shown in figure 4. It is the *negative* regions that result in the severe blurring evident in figure 2 since this corresponds to these spatial frequencies having their contrast reversed.

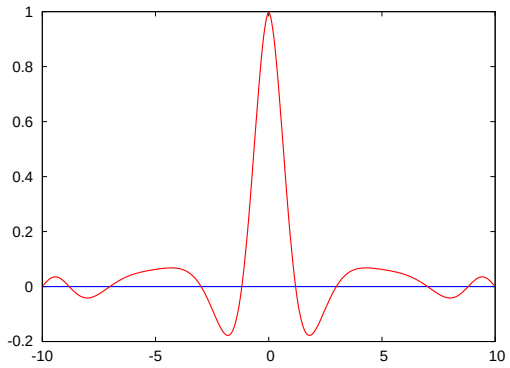

Figure 4: Plot of the optical transfer function associated with defocus showing multiple zeros and negative regions.

The simplest solution to this problem is to modify the inverse filter to to *ignore* the regions where $H(k,l)$ is small and the noise therefore dominates by taking,

$$\begin{aligned} \tilde{F}(i,j) &= \frac{G(i,j)}{H(i,j)} \qquad \text{for } |H(i,j)|^2 > T \\ &= 0 \qquad\qquad \text{for } |H(i,j)|^2 < T \end{aligned}$$

where the threshold T is chosen so than $T \approx |N(i,j)|^2$. We can then form the reconstruction $\tilde{f}(i,j)$ by inverse Fourier transform. The reconstruction of the simulated linear blur shown

in figure 1 is shown in figure 5. The reconstruction is reasonable, but the sharp threshold in Fourier space results in regions of zero in $\tilde{F}(i,j)$ shown in figure 5 (d) which give rise to *ringing* in reconstruction $\tilde{f}(i,j)$ shown in figure 5 (c). This threshold inverse filter can be optimised by careful choice of threshold, but will always still suffer from some ringing which severely limits its use.

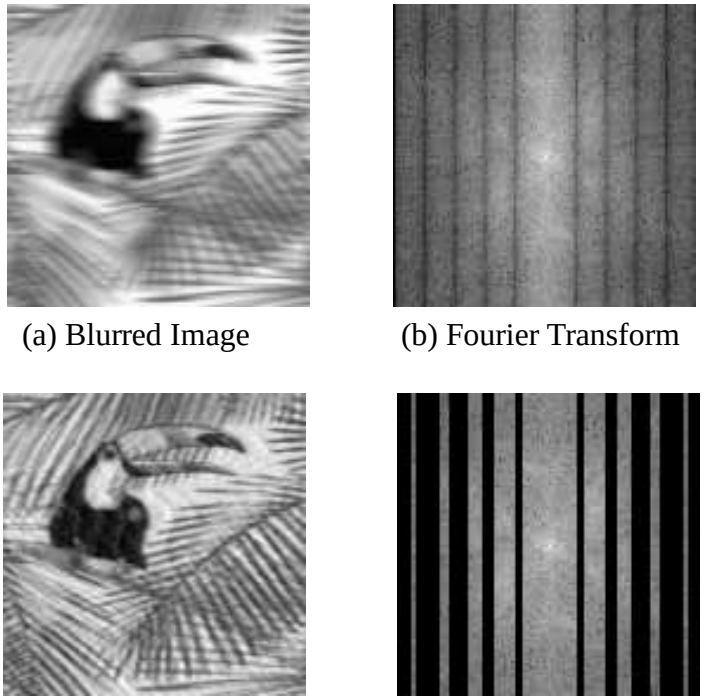

(a) Blurred Image (b) Fourier Transform

(c) Reconstruction (d) Fourier Transform

Figure 5: Threshold inverse filter of the simulated linear blur showing significant ringing.

7.3 Wiener or Optimal Filter

The Wiener filter aim to solve the main problem of control of noise highlighted above by forming a reconstruction that is a *least squares* estimate $\tilde{f}(i,j)$, of the ideal image $f(i,j)$, so that,

$$\left\langle |\tilde{f}(i,j) - f(i,j)|^2 \right\rangle \quad \text{Minimum}$$

which can be *tuned* for different noise levels, and should therefore be applicable for a large range of known point spread functions. To implement this, define an optimal filter $y(i,j)$ such that the least square reconstruction is given by

$$\tilde{f}(i,j) = g(i,j) \odot y(i,j)$$

We also have that the defected image is given by

$$g(i,j) = f(i,j) \odot h(i,j) + n(i,j)$$

The aim is now to find $y(i,j)$, such that the difference between the reconstruction and the ideal image is minimised.

We need to consider this problem in Fourier space where we have that,

$$G(k,l) = F(k,l)H(k,l) + N(k,l)$$

therefore by substitution, we have that the in Fourier space the reconstruction is

$$\tilde{F}(k,l) = G(k,l)Y(k,l) = F(k,l)H(k,l)Y(k,l) + Y(k,l)N(k,l)$$

Since we know that the Fourier transform is unitary, then there is the *same* information in *Real* and *Fourier* space; therefore if two solutions are close together in real space, they will also be close in Fourier space, we can therefore perform the minimisation in Fourier space to give,

$$\left\langle |\tilde{F}(k,l) - F(k,l)|^2 \right\rangle \quad \text{Minimum}$$

where $Y(k,l)$ is the minimisation variable. We know that the minimum[2] will occur when the differential with respect to the minimisation variable is zero, so we therefore have that

$$\frac{\partial}{\partial Y}\left\langle |\tilde{F} - F|^2 \right\rangle = 0$$

which substituting for $\tilde{F}$ gives that

$$\frac{\partial}{\partial Y}\left\langle |F - Y\,H\,F - Y\,N|^2 \right\rangle = 0$$

We can now expand the square, and noting that the noise is independent and zero meaned so that $\langle N \rangle = 0$, we get that

$$\frac{\partial}{\partial Y}\left\langle Y\,Y^*|W|^2 - Y^*H^* - YH + 1 \right\rangle = 0$$

where we have that

$$|W|^2 = |H|^2 + \frac{|N|^2}{|F|^2}$$

We note that Y is complex, so we explicitly write $|Y|^2 = Y\,Y^*$. Now by differentiation, by Y we then get that,

$$\frac{\partial Y^*}{\partial Y}\left\langle \left| Y|W|^2 - H^* \right| \right\rangle + \frac{\partial Y}{\partial Y}\left\langle \left| Y^*|W|^2 - H \right| \right\rangle = 0$$

We note that this is of the form

$$a + a^* = 0$$

so that *both* parts *must* to zero. Now if $Y(k,l) \neq$ Constant[3], then we must have that

$$\frac{\partial Y^*}{\partial Y} \neq 0 \quad \text{and} \quad \frac{\partial Y}{\partial Y} \neq 0$$

which gives a solution for $Y(k,l)$ the optimal filter that minimised the distance between $F(k,l)$ and $\tilde{F}(k,l)$ is given by

$$Y(k,l) = \frac{H^*(k,l)}{|W(k,l)|^2}$$

which, substituting back for $|W(k,l)|^2$ can be written as:

$$Y(k,l) = \frac{H^*(k,l)}{|H(k,l)|^2 + \dfrac{|N(k,l)|^2}{|F(k,l)|^2}}$$

where $||^2$ are the *Power Spectrum*. This gives us the *full solution* to the minimisation, but to actually apply it we need take some assumptions and estimates.

[2] or maximum

[3] the trivial solution

7.3.1 Estimates for the Wiener Filter

The expression for the optimal filter is in terms of $H(k,l)$ the optical transfer function of the system, $|N(k,l)|^2$ the power spectrum of Noise, and also $|F(k,l)|^2$ which is the power spectrum of the *ideal* reconstructed image. In any practical reconstruction system we either know, or can measure the *Point Spread Function:* $h(i,j)$ so we can calculate the *optical transfer function* $H(k,l)$. We are assuming Gaussian Additive noise $n(i,j)$, which gives us that $|N(k,l)|^2 \approx$ Constant, then from Parceval's theorem give us that

$$|N(k,l)|^2 = \sigma_n^2 \quad \text{Variance of Noise}$$

The problem term is $|F(k,l)|^2$ the power spectrum of *ideal* image which clearly we do not know, so have to make approximations. There are a range of possible approximation, these being

1. Smoothed version of $|G(k,l)|^2$, so the power spectrum of the detected image. This is valid provided that $H(k,l)$ has no zeros, however in most practical cases, such as defocus or linear blur, $H(k,l)$ *does* have multiple zeros, so this scheme does not work.

2. Approximate $|F(k,l)|^2$ by *Negative Exponential*. This assumes that the image is fractal consisting of a series of repeating shape at ever decreasing scale. This is a reasonable model for many natural scenes such as aerial photographs but numerically there are problems close to $(0,0)$).

3. Approximate $|F(k,l)|^2$ by a Gaussian which is the mathematically easy solution that corresponds to a *typical* power spectrum with most power at low frequencies.

4. Take $|F(k,l)|^2 \approx$ constant, which initially look a very poor model since it actually assumes that the image is uncorrelated random noise.

In practice quality of reconstruction only weakly dependent on function form taken for $|F(k,l)|^2$ and in most cases the apparently crudest of it being *constant* gives the best results. Given this the Wiener Filter is frequently written as

$$Y(u,v) = \frac{H^*(k,l)}{|H(k,l)|^2 + \dfrac{1}{\text{SNR}^2}}$$

where SNR is chosen to give the best visual reconstruction.

The result of applying this filter to the linear blur shown in figure 1 and defocus shown in figure 2 is shown in figure 6 using SNR $= 1000$ which is equivalent to *no noise*. This shown essentially perfect reconstructions and their associated Fourier transforms shown none of the sharp discontinuities evident in the thresholded inverse filter. In the Fourier plane of the defocus reconstruction there is some evidence of low-pass filtering due to $H(k,l)$ being very small at high spatial frequencies, but it still gives an excellent reconstruction.

7.3.2 Effect of SNR on Reconstruction

The exact effect of the SNR term in the Wiener filter construction will depend on the shape $H(k,l)$ of the system. but we can gain insight by considering the specific and typical case of

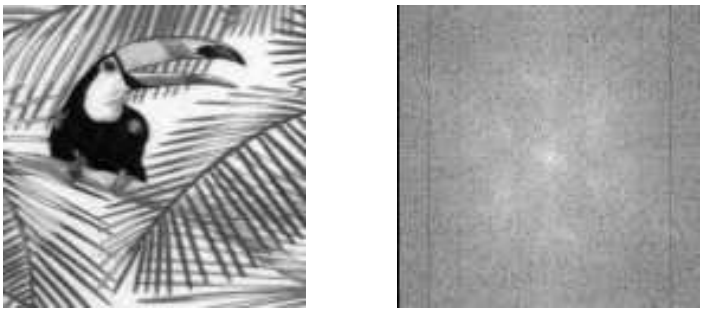

Linear Blur Fourier Transform

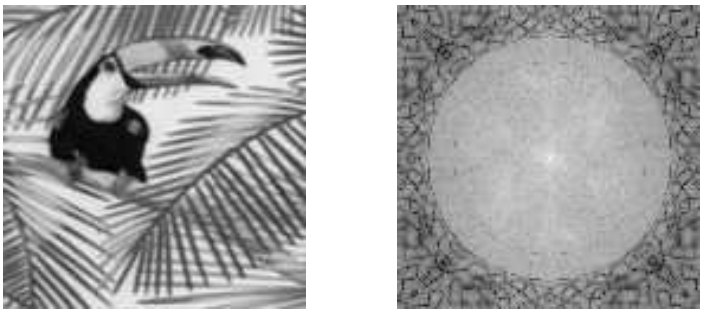

Defocus Image Fourier Transform

Figure 6: Low noise Wiener filter reconstructions of linear blur and defocus.

defocus of a square[4] lens. This is shown in detail in figure 7, where the the OTF, $H(u)$ is shown in 7 (a) being the same transfer function used in the previous defocus examples with severe attenuation of high spatial frequencies, multiple zeros and regions of contrast reversal. The shape of $Y(u)$ the Wiener filter is plotted in 7 (b) to (d) for SNR in range $1 \rightarrow 256$. At low SNR is filter correct the regions of negative contrast, so will correct the worst aspects of the blurring, but does little to enhance the high spatial frequencies, while at high SNR is the high spatial frequencies as also enhanced. This is as expected, since at low SNR the image will be severely corrupted with noise which has most effect at high spatial frequencies, so enhancement of these high frequencies will simply enhance the noise. Similarly at high SNR there is little noise so it is *safe* to enhance the high spatial frequencies.

We can consider the overall effect of *blur* plus *reconstruction* since in Fourier space, ignoring noise, the reconstruction is is given by

$$\tilde{F}(k,l) = Y(k,l)\,G(k,l) = (Y(k,l)\,H(k,l))\,F(k,l)$$

so the overall effect of of blurring the image and then reconstruction with the Wiener filter is given by by $Y(k,l)\,H(k,l)$, which can be plotted for a range of SNRs as is shown in figure 8. This shown, in figure 8 (a) that at low SNR the combination acts like a low pass filter which severely attenuates the high spatial frequencies, so will significantly blur the image edges. As the SNR rises the low pass effect reduces, so that in figure 8 (c) the effect of the blur and reconstruction is almost flat except for the regions where $H(u) \rightarrow 0$ where the information is totally lost in the initial blur, and is therefore also lost in the reconstruction. These graphs show that the Wiener filter is *well behaved* at all SNR introducing a *low pass* effect when the images

[4]The results for a more conventional circular lens are almost identical but $H(k,l)$ is a much more complex expression.

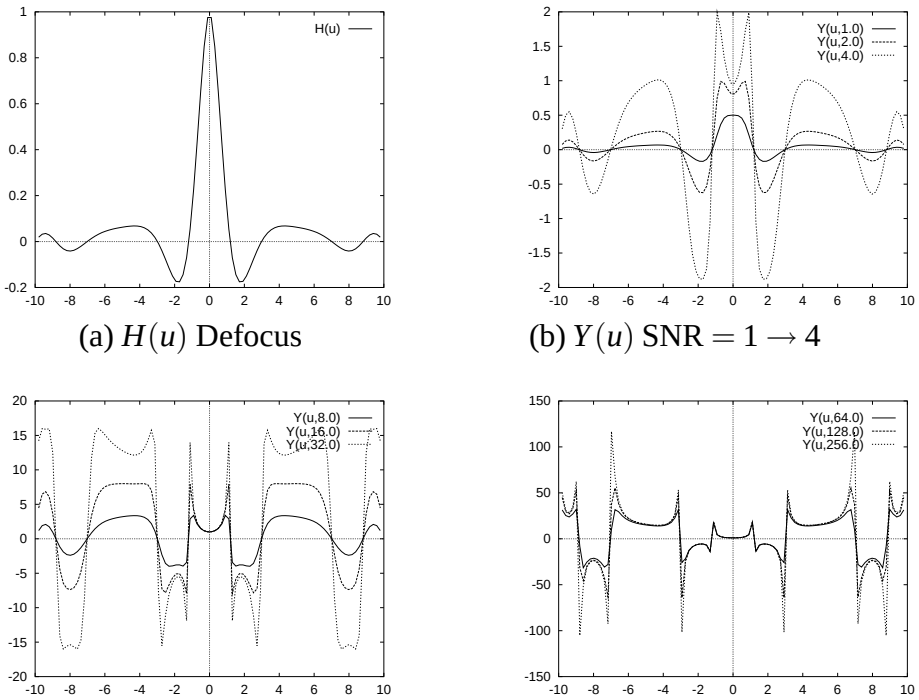

(a) $H(u)$ Defocus (b) $Y(u)$ SNR $= 1 \rightarrow 4$

(c) $Y(u)$ SNR $= 8 \rightarrow 32$ (d) $Y(u)$ SNR $= 64 \rightarrow 256$

Figure 7: Shape of Wiener filter for defocus at various SNR,

is noisy to prevent amplification of noise in the reconstruction, while at high SNR enhances all available information back to as close as possible to the original, ideal image.

7.3.3 Modified Wiener Filter

We have seen above that for low(ish) SNR the Wiener Filter acts as a low pass filter that will tend to blur edges, so we can consider trying to add an additional constraint the the minimisation to counteract this effect. For and image $f(x,y)$, we have,

$$\frac{\partial f(x,y)}{\partial x} = \mathcal{F}^{-1}\{uF(u,v)\} \quad \text{and} \quad \frac{\partial f(x,y)}{\partial y} = \mathcal{F}^{-1}\{vF(u,v)\}$$

so that

$$|\nabla f(x,y)| = \mathcal{F}^{-1}\{wF(u,v)\} \quad \text{where} \quad w = \sqrt{u^2+v^2}$$

where we have already seen that $|\nabla f(x,y)|$ is a high-pass version of the image, so enhancing the edged.

So to enhance edges, while removing the blur we can modify minimisation in Fourier space to

$$\langle|\tilde{F}(u,v) - F(u,v)|^2\rangle + \lambda\langle|w\tilde{F}|\rangle$$

This "can be shown" give,

$$Y(u,v) = \frac{H^*}{|W|^2}\left(\frac{1}{1-\lambda\frac{w^2}{w_0^2}}\right)$$

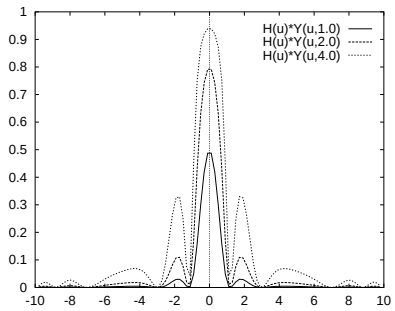

(a) $H(u)Y(u)$ SNR $= 1 \rightarrow 4$

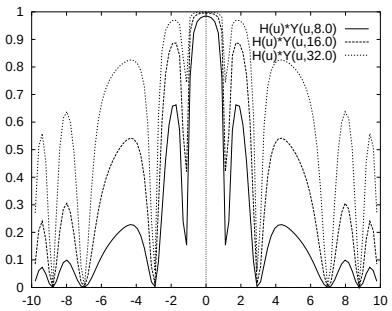

(b) $H(u)Y(u)$ SNR $= 8 \rightarrow 32$

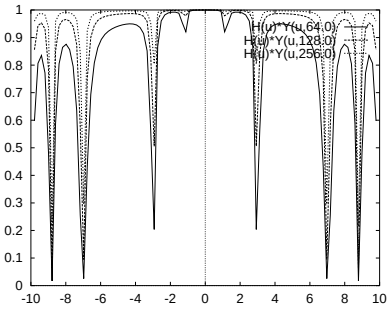

(c) $H(u)Y(u)$ SNR $= 64 \rightarrow 356$

Figure 8: Overall effect of blur and reconstruction at a range of SNR

where w_0 is the band-limit of the reconstruction system, and λ is range ± 1. We therefore have,

$$\begin{aligned} \lambda \quad &= 0 \quad \text{Unconstrained Wiener} \\ &> 0 \quad \text{Edges enhanced Wiener} \\ &< 0 \quad \text{Edges reduced Wiener} \end{aligned}$$

In practical cases the effect of varying λ will depend in the form of $H(u,v)$ and the SNR. This modification gives a useful extra parameter to optimise but if used to excessively enhance edges when SNR is low results in significant enhancement in the noise.

7.4 The CLEAN Algorithm

The inverse and wiener filters are both linear Fourier space filters which assume the degraded image contains all the information about the ideal image but it has been *scrambled* by a known point-spread function. If however the degraded image is as a result of areas of the Fourier space missing, such as found in tomography or radio astronomy, then the linear filters will not produce any sensible reconstruction and we have to consider alternative schemes.

A typical scenario is shown in figure 9 which shown an ideal star image in figure 9 (a) and its Fourier transform in 9 (b). If the data is collected in Fourier space[5] over a limited region, in this case half the Fourier plane in a *bow-tie* pattern as shown in 9 (c), then the collected image is as shown in 9 (d) showing considerable artifacts including the stars being elongated and spurious ringing effects.

The simplest scheme to deal with this type of reconstruction is the CLEAN algorithm originally designed to deal with radio astronomy data. We can assume the image consists of a collection

[5] See next section on tomography.

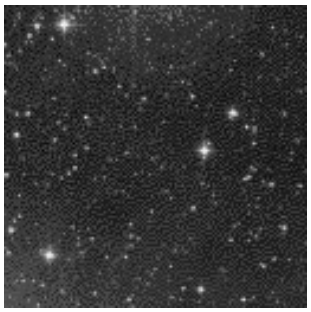

(a) Star Image

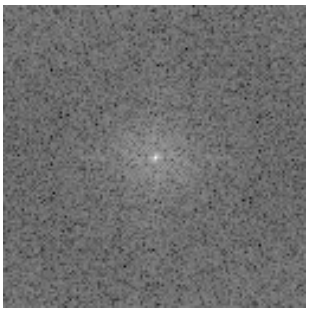

(b) Fourier Transform

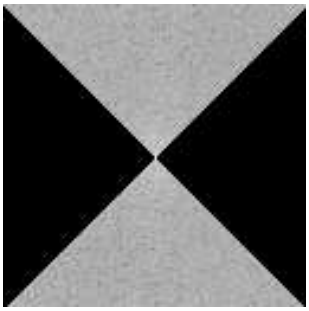

(c) Collect FT space

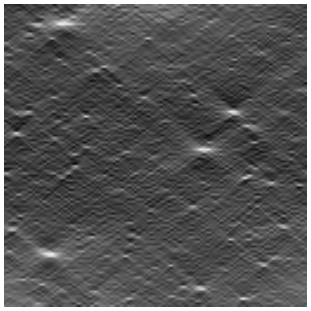

(d) Collected Image

Figure 9: Result of simulation where large sections of the Fourier plane are removed showing a degraded image.

of isolated *stars* convolved with a point spread function as shown in figure 10. The aim of the CLEAN is searches for point spread functions in real space input image and *replaces* them by *stars*, or δ−functions in the output image.

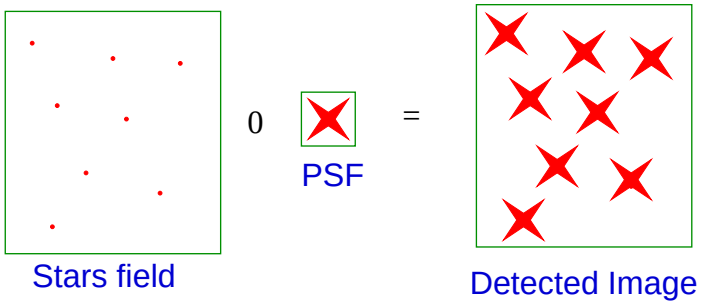

Figure 10: Model behind the CLEAN algorithm.

Assume that PSF is sharply peaked in the centre, then the CLEAN scheme is simply implemented by, then scheme is:

1. Locate Maximum value in image.
2. Record location and height of PSF.
3. Subtract scaled PSF from image at that location.
4. If any peaks left, go to (1)

Looks *very* simple, but does it work provided the imaging system matches the underlying model.

To get this to actually work well, we need to add a variable scaling parameter when subtracting the point-spread function, you typically remove 80% of the maximum peak found, and you also need care in when to stop stop searching for more peaks, typically when the peaks left are comparable with the variance of the noise. Reconstruction of the degraded image from figure 9 is shown in figure 11 with the point-spread function shown in 11 (b) and the reconstruction in 11 (c) which consists of a set of $\delta-$functions. Examining the Fourier transform of the reconstruction in 11 (c) shown that data has been *interpolated* into the two blank regions in the Fourier transform of the collected data shown in 9 (c), that that we get a consistent image which differs significantly from the linear filtering processes such as the Wiener filter which would have left these regions blank. The final reconstruction is usually smoothed by convolution with a Gaussian to give the reconstruction in 11 (e) which smooths out the isolated spikes making the image easier to understand.

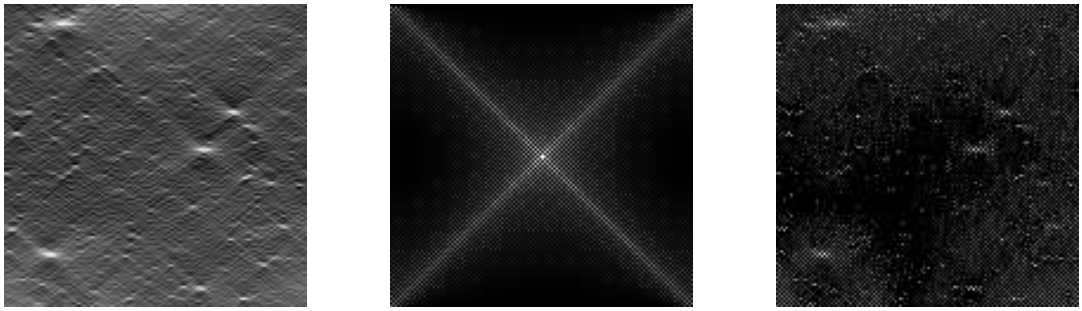

(a) Collected Image (b) PSF (stretched) (c) Reconstruction

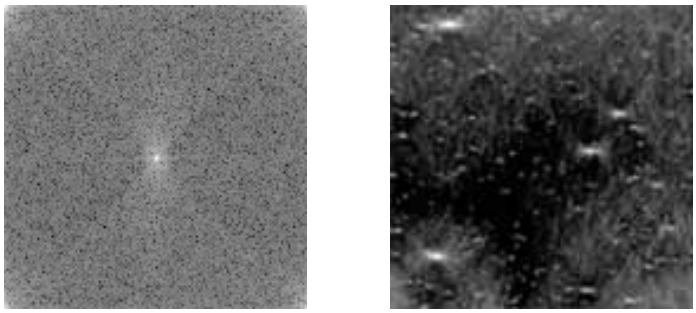

(d) FT of Reconstruction (e) Gaussian Low-pass

Figure 11: Example of reconstruction using the CLEAN algorithm.

7.5 Maximum Entropy

One of the most powerful reconstruction schemes is to maximise the *entropy* of reconstruction subject to certain constraints, usually that it closely matches the ideal detected image. This has the effect of producing the *smoothest* image consistent with the observed data. To see this consider the definition of entropy being, of a two dimensional image as begin

$$H_f = -\langle p(i,j) \log p(i,j) \rangle$$

where

$$p(i,j) = \frac{f(i,j)}{N^2\langle f(i,j)\rangle}$$

which can be considered as a *probability* since it is normalsied with

$$\sum_{i=1}^{N}\sum_{j=1}^{N} p(i,j) = 1$$

Let us initially maximise H_f simply subject to the constraint that the summation over the image is constant[6]. Consider two pixels locations at k,l and m,m with $p(k,l)$ & $p(m,n)$ as shown in figure 12. If we move an amount Δ from one to the other, so that

$$\begin{aligned} p(k,l) &\rightarrow p(k,l)-\Delta \\ p(m,n) &\rightarrow p(m,n)+\Delta \end{aligned}$$

then provided that Δ is small, we can find the effect of H_f as can shown to be

$$H'_f = H_f + \Delta\log\left(\frac{p(k,l)}{p(m,n)}\right)$$

so that

$$H'_f > H_f \quad \text{iff } p(k,l) > p(m,n)$$

So by *reducing* peaks and *increasing* troughs the maximise H_f. If this processes is continued, then the global maximum must be where there are no *peaks* or *troughs*, so when

$$p(i,j) = \text{constant} = \frac{1}{N^2}$$

which corresponds to the *smoothest possible image* given the simple constraint. This simple example illustrated that maximising *entropy* has the effect of smoothing the image.

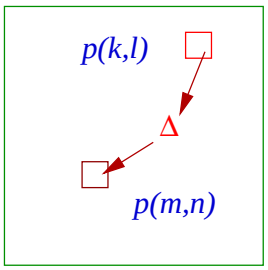

Figure 12: Maximise the entropy subject to the pixel summation being constant.

7.5.1 More Practical Entropy

A more flexible and practical scheme uses an alternative definition of *entropy* of an image $f(i,j)$ being,

$$H_f = -\langle f(i,j)\ [\log(f(i,j)/A) - 1\ ]\rangle$$

where A is the *average* brightness background intensity of the image. This definition has similar mathematical properties to the conventional statistical physics definition of *entropy* but with *two* important differences differences.

[6] We will consider more realistic constraints shortly.

1. Normalisation constraint removed, which now is typically incorporated in constraints on reconstruction.

2. Free parameter A to characterise image.

This alternative definition is more applicable to real systems.

7.5.2 Max Entropy Deconvolution

The most common use of the *maximum entropy* is as a constrain in deconvolution of a point-spread function in the presence of noise with the aim of producing the *smoothest* image consistent with the observed data. In addition the log() in the expression also has the additional useful property of forcing the reconstruction to be positive[7].

The usual image model is just

$$g(i,j) = h(i,j) \odot f(i,j) + n(i,j)$$

If the reconstruction is given by $\tilde{f}(i,j)$, then the *ideal* detected image, without the effect of noise, must be given by,

$$\tilde{g}(i,j) = h(i,j) \odot \tilde{f}(i,j)$$

so for $\tilde{f}(i,j)$ to be a valid reconstruction, $\tilde{g}(i,j)$ must closely approximate $g(i,j)$. One possible measure is the least squares difference being

$$E = \left\langle \frac{|\tilde{g}(i,j) - g(i,j)|^2}{\sigma_n^2} \right\rangle$$

where σ_n^2 is variance of the noise, so the more noise we expect in the system the more the variation that is allowed. So to get the *maximum entropy* reconstruction subject to it being a *valid reconstruction* we can found by maximisation of

$$Q(\tilde{f}) = H(\tilde{f}) - \lambda E(\tilde{f})$$

where λ is a constant used to control the reconstruction.

This relation does not have a analytical solution but *can be shown* to be solvable digitally by steepest decent to give iterative scheme of

$$\tilde{f}^{k+1} = \tilde{f}^k + A \exp\left[-\frac{2\lambda}{\sigma_n^2} h \odot (\tilde{g}^k - g) \right]$$

where we have that

$$\tilde{g}^k = h \odot \tilde{f}^k$$

This scheme require $h(i,j)$ the point-spread function, σ_n^2, the variance of the noise, A the image background, and f^0 the starting image condition, to be known typically where we typically take as $f^0 = A$ a constant as the starting condition. A typical example is shown in figure 13 where the car number plate is severely blurred in the original image are clearly readable in the reconstruction.

[7] This is often a problem in linear filters, such as the Wiener filter, where ringing can result in negative regions in the reconstruction.

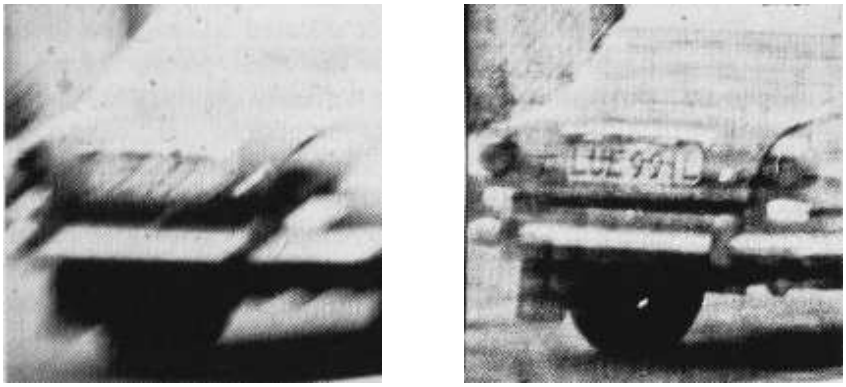

Figure 13: Example of maximum entropy deconvolution from from Skilling et al. Cambridge.

Maximum entropy is a computationally very heavy algorithm with two convolutions per iteration, and typically many hundreds of iterations to form a reconstruction. This scheme is also difficult to make numerically stable, and in practice the A value and λ in the definition of *entropy* have to be carefully controlled and modified throughout the iterations to give a sensible solution. On more significance is that in practice this algorithm will converged to a *good* and plausible solution even if $h(i,j)$ is NOT well known making it the ideal choice for reconstruction when the details of the imaging system are not precisely known.

7.6 Geometric Image Correction

Many imaging system suffer from geometric distortion. This can be as a result of aberrations in the imaging system, for example with ultra-wide angle lenses straight lines are images as curves, or as a result of the geometry of the imaging systems, for example a satellite image of the curved Earth. In all such cases the system now has a *space variant* PSF with different imaging characteristics is different part of the image, so these is no deconvolution based reconstruction scheme and other methods have to be found.

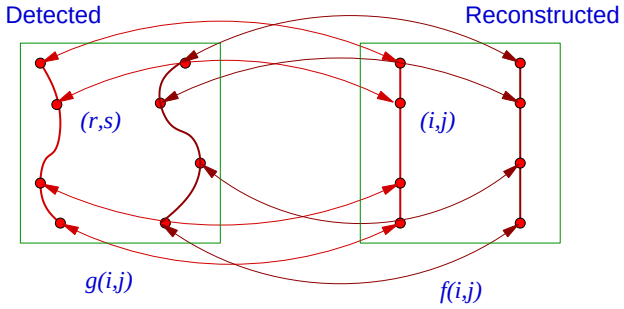

Figure 14: Re-sampling of a geometric distorted image.

Consider problem as *two-dimensional curve fitting* onto a non-linear sampling grid. If the detected image is $g(i,j)$ then we define two *distortion functions* $r(i,j)$ & $s(i,j)$, such that, as shown in figure 14, the *ideal* image is

$$f(i,j) = g(r,s)$$

This formulates the problem as re-sampling $g(i,j)$ on a grid defined by $r(i,j), s(i,j)$

Before considering how to calculate the re-sampling functions $r(i,j), s(i,j)$, consider their functional form. If the geometric distortion is only *translation* then we simply have

$$r = i + a_0 \quad \text{and} \quad s = j + b_0$$

which for the more general case of *translation, scale* & *Rotation*, we need six parameters giving,

$$r = a_0 + a_1 i + a_2 j \quad \text{and} \quad s = b_0 + b_1 i + b_2 j$$

which will give the type of linear warp as shown in figure 15.

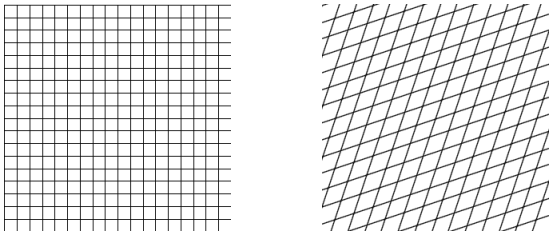

Grid Image Linear Warp

Figure 15: Example of a linear warp characterised by six parameters.

A simplest example of a linear warp is an image rotation where from a rotation of θ the parameters are

$$a_1 = \cos\theta \qquad b_1 = -\sin\theta$$
$$a_2 = \sin\theta \qquad b_2 = \cos\theta$$

which is shown in figure 16 applied to the `toucan` image for $\theta = 30^\circ$.

Figure 16: Rotated version of the toucan with $\theta = 30^\circ$.

The next level of geometric correction to correct to geometric distortions of *skewing* have 12 parameters giving expression for $r(i,j), s(i,j)$ given by,

$$\begin{aligned} r &= a_0 + a_1 i + a_2 j + a_3 i^2 + a_4 j^2 + a_5 ij \\ s &= b_0 + b_1 i + b_2 j + b_3 i^2 + b_4 j^2 + b_5 ij \end{aligned}$$

which give non-linear warping as shown in figure 17. This is also scheme used in computer graphics to wrap and image round a three-dimensional object. It is also possible to go to higher order and to include cubic terms which results in 20 parameters. This is not commonly used since in most practical cases good results can be obtained with the simpler 12 parameter model.

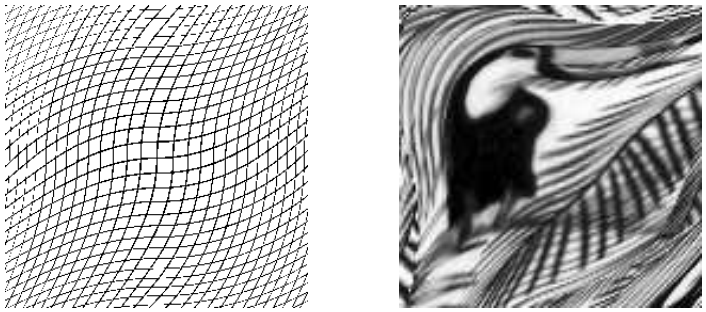

Figure 17: Grid and toucan image after warping with twelve parameter non-linear geometric correction functions.

7.6.1 Calculation of Geometric Distortion Parameters

In some cases, where the optical imaging system is well known, it is possible to calculate parameters directly from the system design. This was possible in old video cameras where the detection tube had a curved front, or for a satellite is in an known orbit with respect to the Earth, for example a geostationary weather satellite forming an image of the whole Earth disc and we want to form a geometrically correct image of UK.

In most cases we do not know the distortions analytically and they have to be found from the distorted image. To do this we assume we can locate *M known* features with locations

$$(r_k, s_k) \quad k = 1, \ldots, M$$

while we assume that their *true* locations are at,

$$(i_k, j_k) \quad k = 1, \ldots, M$$

as shown in figure18. So if the warping parameters are correct then we have that

$$r(i_k, i_k) = r_k \quad s(i_k, j_k) = s_k$$

which is a set of coupled non-linear equations which can be used to calculate the a_i and b_i.

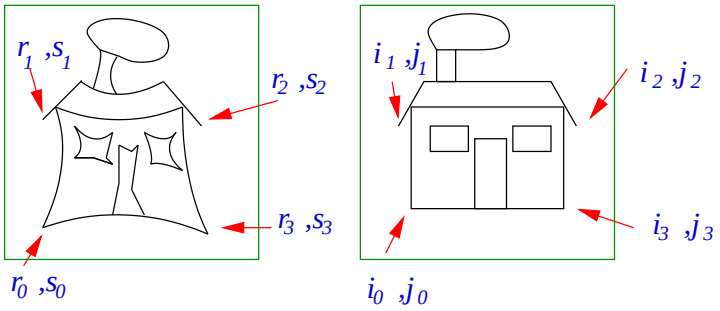

Figure 18: Location of known features are their true locations is a geometrically distorted image.

In practice it is better to measure *many points* on the image and estimate parameters by minimisation of the least square errors given by

$$e_a^2 = \sum_{k=1}^{M} \left(r_k - r(i_k, j_k) \right)^2 \quad \text{and} \quad e_b^2 = \sum_{k=1}^{M} \left(s_k - s(i_k, j_k) \right)^2$$

Clearly for a 12 parameters kit a *minimum* of 12 points are needed but usually take more than 100 points spread over the *important* regions of the image. This techniques is widely used in satellite data and preparation of images for automatic map making with either manual or automated location of the control points.

7.7 Re-sampling Procedure

To implement geometric correction we require to be able to form

$$f(i,j) = g(r(i,j), s(i,j))$$

where, in general $r(i,j)$ and $s(i,j)$ will not be integers so will not fall on grid points, so must interpolate between grid points from a continuous approximation of the detected image. We know, from previous that the continuous approximation given by

$$g(x,y) = h(x,y) \odot g(i,j)$$

where $h(x,y)$ is the interpolation function. In most practical systems either *zero* or *first* order interpolation, being either the value of the closest pixel or the weighted of the four nearest neighbours. This can result is some aliasing which can be evident in the Fourier transform of the geometric corrected. The Fourier transform of the rotated image in figure 16 is shown in figure 19. The rotation used *zero* order interpolation in real space which results in a stray horizontal bright band and some evidence of a vertical band thought the centre of the Fourier transform.

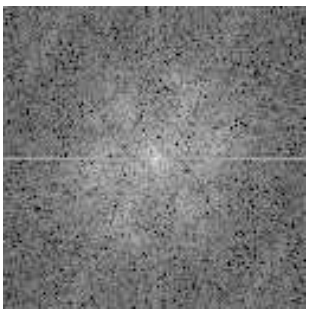

Figure 19: Fourier transform of the rotated toucan image shown re-sampling error only the horizontal.

In addition in many practical cases values of $r(i,j)$ & $s(i,j)$ may be outside the known range of the detected image data, so for a $N \times N$ image may be outside the range $0 \rightarrow N-1$. There are two possible solutions to this, being

1. *Cyclic Wrap round* where we assume the

$$g(N+i, N+j) = g(i,j)$$

although *correct* from a sampling viewpoint, frequent odd results obtained as shown in figure 20 where the toucan image is repeated in two dimensions.

2. *Zero Pad* where we assume that

$$g(r,s) = 0 \; r \text{ or } s \text{ outside image}$$

   which will give spurious boarder of *zero* round parts of image, has to be allowed for, especially if then processed by edge detectors.

So either solution is ideal, they both have different errors.

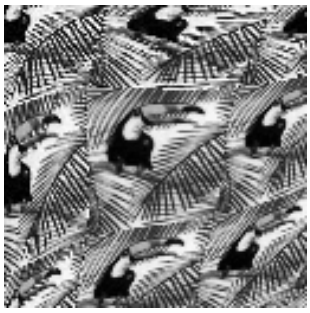

Figure 20: Effect of cyclic wrap round in two dimensions

7.8 Summary

In this long section we have covered

1. Inverse Filtering
2. Optimal or Wiener Filter
3. CLEAN reconstruction.
4. Maximum Entropy Reconstruction
5. Geometric Image Correction

Workshop Questions

7.1 Shape of $H(k,l)$ for linear blur

For a 256 by 256 image convolved with a linear blur with a length of M pixels, calculate the analytical expression for $H(k,l)$. Sketch this function and discuss how the first zero is located to the length of the linear blur.

7.2 Wiener Filter Simulation

Try the `wiener` filter simulation programme to experiment with the effect of noise levels and SNR parameter in the Wiener Filter.

The program is based on linear horizontal blur PSF and operates as follows:

1. Initially asked for an input "ideal" image. The `toucan.pgm` is a good start.
2. Asks for size of horizontal blur in pixels. Blur function is a horizontal line of the specified length, 1 pixel wide. (Try 10 to 20 pixels).
3. Optionally adds Gaussian signal dependent noise to give a specified SNR. The added noise has standard deviation,
$$\sigma_n = \frac{\sigma_f}{SNR}$$
where σ_f is calculated from the input image.
4. The output image is then displayed. (due to buffering they may be delayed).
5. The SNR used in the wiener filter is then asked for. Note: Your should experiment by changing the SNR to values other than that used in the noise, in particular what happens if the wiener SNR is too high?
6. The reconstruction is then displayed